Impact of Meteorological factors on wheat growth period and irrigation water requirement —A case study of the Beijing-Tianjin-Hebei region in China

* Chengcheng Xu [1,2], Chuiyu Lu [2], Jianhua Wang [2]

(1. School of Earth and Environment, Anhui University of Science and Technology, Huainan: 232001, China;

2. State Key Laboratory of Water Cycle Simulation and Regulation, China Institute of Water Resources and Hydropower Research, Beijing: 100038, China)

Corresponding Author: Chengcheng Xu, Email address: 1647203047@qq.com

Abstract: This study analyzes the irrigation water requirement of wheat in the growth stage in the Beijing-Tianjin-Hebei region under the changes of meteorological factors conditions, using the growth period data, and meteorological data from 80 meteorological stations, from 2000 to 2019. The results show that: (1) The annual average precipitation, average wind speed, and average relative humidity of the growth period in the Beijing-Tianjin-Hebei region show a downward variation trend, while the temperature variation shows an upward trend. Moreover, relative humidity and radiation exhibit a negative spatial correlation. (2) Wheat irrigation water requirement in the Beijing-Tianjin-Hebei region gradually decreases from north to south and east to west. However, the eastern region shows a gradually increasing trend, while the western region shows a decreasing trend. (3) Meteorological factors are negatively correlated with irrigation water requirement, potential evapotranspiration, effective precipitation, and relative humidity, and significantly positively correlated with sunshine hours, average temperature, and wind speed. The overall variation in irrigation water requirement has the highest correlation with potential evapotranspiration. However, the yearly variations in regional irrigation water requirement are dependent on factors such as wind speed, relative humidity, and radiation.

Keywords: wheat growth period; meteorological factors; irrigation water requirement; China.

1. Introducion

The United Nations defines climate change as the variation in the Earth's atmospheric composition from direct or indirect human activities, in addition to the natural variability of climate observed during similar periods. The impact of climate change on the human environment has

29 increased progressively and extensively (Seo et al., 2013; Ju et al., 2013; Calzadilla et al., 2013;
30 Noufé et al., 2015), and since the First World Climate Conference in 1979, climate change research
31 has gradually attracted global attention (Iglesias, 2012; Ahmad et al., 2019; Mayank et al., 2019;
32 Pons et al., 2020). The World Meteorological Organization (WMO) and the United Nations
33 Environment Programme (UNEP) are two major organizations dealing with climate change, that
34 simultaneously established the Intergovernmental Panel on Climate Change (IPCC) (Van der and
35 Warner, 2020). The various assessment reports put forward by the IPCC since 1990 have established
36 a scientific basis for climate change research, by indicating that global warming was caused by both
37 natural and manmade factors. The global temperature reportedly rose by 0.3-0.6 °C in a century.
38 Furthermore, the elevation in global average temperature since the mid-20th century was primarily
39 attributed to greenhouse gases emitted through human activities. The global climate change since
40 the past 132 years (1880-2012) was also elaborated. Moreover, the IPCC 2013 report predicts the
41 trend of climate change at the end of the 21st century through a variety of scenario models:
42 Temperature rise varies regionally, and it will be higher on the land than the sea by 1.4-1.7 °C, with
43 the Arctic recording the highest temperature (McBride et al., 2020). Extreme hot weather events
44 will increase, and the duration will be lengthened in most areas, and extreme cold weather events
45 will decrease. The frequency of high temperature events will double every two decades. Increased
46 precipitation will occur mostly in high latitudes and some in mid latitudes, instead of the subtropics.
47 Precipitation will increase with the rise in global warming, and the rate of increase in precipitation
48 for a unit temperature rise is less than that of water vapor. Precipitation will show high spatial
49 variations, further increasing the precipitation gap between arid and humid regions (Weerathunga
50 et al., 2020), and in most parts of the world, between wet and dry seasons. In addition, precipitation
51 will increase in the equatorial Pacific, high latitude and humid mid-latitude regions and decrease in
52 subtropical and arid mid-latitude regions.

53 The agriculture industry is most vulnerable to the effects of climate change (Sun et al., 2013;
54 Schönhart et al., 2016; Liu et al., 2016). Therefore, the impact of climate change on agricultural
55 production is a relevant issue in climate change research (Dong et al., 2019). Climate change in
56 China follows a similar trend as the overall global climate change, with slight variations (Lv et al.,
57 2013; Zhang et al., 2016). The North China plain is one of the principal wheat producing areas in

China. Climate change inevitably impacts the growth period and water requirement of wheat, thereby affecting its yield and quality (Chen et al., 2013; Wang et al., 2014; Geng et al., 2019; Wang et al., 2019). Thus, the study of regional changes in irrigation water requirement for wheat in the Beijing-Tianjin-Hebei region is significant in relation to the overall temperature rise in North China. Furthermore, the factors affecting wheat irrigation water requirement have also been investigated.

2. Materials and methods

2.1 Overview of the study area

The Beijing-Tianjin-Hebei region (total area of 216,500 km^2), is the "capital economic circle" of China and accounts for 2.3% of the total area of the country. In addition to Beijing and Tianjin, the region comprises Baoding, Langfang, Shijiazhuang, Tangshan, Handan, Qinhuangdao, 11 prefecture-level cities including Zhangjiakou, Chengde, Cangzhou, Xingtai, and Hengshui, and 2 provincial-level cities directly under the control of Dingzhou and Xinji, of the Hebei province. The Taihang Mountains lie to the west, and the Bohai Bay to the east of the Beijing-Tianjin-Hebei region. The terrain is high in the northwest and north, and flat in the south and east (Zhang et al., 2020). In winter, the cold and snowless weather is controlled by the Siberian continental air mass, and northerly and northwestern winds prevail. Spring is affected by the Mongolian continental air mass, such that there is a rapid temperature rise, high wind speed (Guo et al., 2020), dry climate, and amount of evaporation. The weather tends to be dry, windy, and sandy (Guo et al., 2020). Summer is affected by oceanic air masses, and is humid, with high temperatures, and heavy rainfall (Song et al., 2020). However, the inconsistencies in time, intensity, and range of influence of the Pacific subtropical high every summer result in high rainfall variation and occasional droughts and floods. In autumn, the weather is high and the rainfall is low (Zhenyu et al., 2019; Men et al., 2020; Bi et al., 2020).

In the Beijing-Tianjin-Hebei region, 13 main single crops are cultivated, including wheat, corn, cotton, vegetables, potatoes, peanuts, millet, soybeans, forest fruits, and rice. Multiple cropping occupies a part of the region, and is observed primarily for wheat and corn, in addition to wheat and peanuts, soybeans and cotton, cotton and vegetables, and cotton and fruits. Other types of crops such as rape, flax, naked oats, and sorghum, are also cultivated in small areas. However, wheat and corn are the primary plantations occupying a large portion of the Beijing-Tianjin-Hebei region.

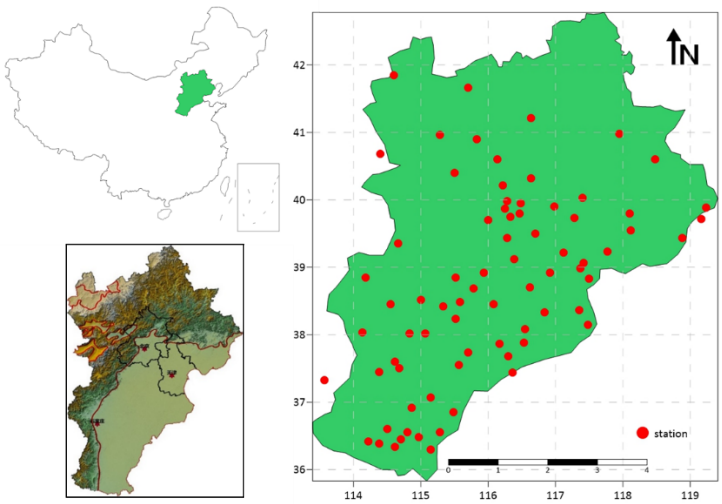

Figure 1 (a) Map showing geographical location of the study area and (b) Map showing distribution of meteorological stations

2.2 Source of information

The meteorological data were obtained from the National Meteorological Center of China. Daily meteorological data, including average temperature (℃), maximum temperature (℃), minimum temperature (℃), sunshine hours (h), precipitation (mm), wind speed (m/s), and average relative humidity (%) were selected from 80 representative ground weather stations from 2000 to 2019. For unavailable meteorological data, the missing values of temperature (average, maximum, and minimum) and precipitation were interpolated using Kriging interpolation.

The growth period data for wheat was obtained from the Chengde, Tangshan, Zunhua, Baoding, Shijiazhuang, and Botou observation stations from 2000 to 2019. Since the growth period observation stations and ground weather stations (Beijing Station, Tianjin Station, Shijiazhuang Station, and Nangong Station) were not consistent, the nearest matching principle was adopted and 80 sets of continuous 20-year observation data were selected, as shown in Table 1.

105 **Table 1 Data of Beijing-Tianjin-Hebei meteorological stations**

NO.	name	province	longitude	latitude	NO.	name	province	longitude	latitude
1	Anguo	Hebei	115.3330	38.4167	41	Funing	Hebei	119.2330	39.8833
2	Anping	Hebei	115.5170	38.2333	42	Fucheng	Hebei	116.1670	37.8667
3	Anxin	Hebei	115.9330	38.9167	43	Fuping	Hebei	114.1830	38.8500
4	Anyang	Hebei	114.1214	36.1427	44	Gangzi	Hebei	118.3119	42.5781
5	Balihan	Hebei	118.6415	41.5130	45	Gaobeidian	Hebei	115.8740	39.3266
6	Bszhou	Hebei	116.3833	39.1167	46	Gaoyang	Hebei	115.7830	38.6833
7	Baixiang	Hebei	114.6830	37.5000	47	Gaoyi	Hebei	114.6170	37.6000
8	Baodi	Tianjin	117.2830	39.7333	48	Gaocheng	Hebei	114.8330	38.0167
9	Baoding	Hebei	115.5167	38.8500	49	Guyuan	Hebei	115.7000	41.6667
10	Beichenqu	Tianjin	117.1170	39.2167	50	Guan	Hebei	116.2830	39.4333
11	Beijing	Beijing	116.4667	39.8000	51	Guantao	Hebei	115.2830	36.5500
12	Botou	Hebei	116.5500	38.0833	52	Guangping	Hebei	114.9670	36.4833
13	Cangzhou	Hebei	116.8333	38.3333	53	Guangzong	Hebei	115.1500	37.0667
14	Changli	Hebei	119.1670	39.7167	54	Haidian	Beijing	116.2830	39.9833
15	Changping	Beijing	116.2170	40.2167	55	Haixing	Hebei	117.4830	38.1500
16	Chaoyang	Beijing	116.4830	39.9500	56	Handan	Hebei	114.5000	36.6000
17	Chengan	Hebei	114.7000	36.4500	57	Hanguqu	Tianjin	117.7670	39.2333
18	Chengde	Hebei	117.9500	40.9833	58	Xingtang	Hebei	114.5500	38.4500
19	Chicheng	Hebei	115.8330	40.9000	59	Linzhang	Hebei	114.617	36.3333
20	Congli	Hebei	115.2830	40.9667	60	Hejian	Hebei	116.083	38.45
21	Cixian	Hebei	114.3830	36.3833	61	Hengshui	Hebei	115.7000	37.7333
22	Dachang	Hebei	116.9833	39.9000	62	Huaian	Hebei	114.4000	40.6833
23	Dacheng	Hebei	116.6170	38.7000	63	Huailai	Hebei	115.5000	40.4000
24	Dagangqu	Tianjin	117.5000	38.8333	64	Huairou	Beijing	116.6330	40.3167
25	Daming	Hebei	115.1500	36.3000	65	Haungye	Hebei	117.3500	38.3667
26	Daxing	Beijing	116.3330	39.7500	66	Jize	Hebei	114.8670	36.9167
27	Dezhou	Hebei	116.3590	37.4355	67	Jixian	Tianjin	117.4000	40.0333
28	Dingzhou	Hebei	115.0000	38.5167	68	Jixian	Hebei	115.5670	37.5500
29	Dongguang	Hebei	116.5330	37.8833	69	Jinqu	Tianjin	117.3670	38.9833
30	Dongli	Tianjin	117.4170	39.0667	70	Jinxian	Hebei	115.0670	38.0167
31	Duolun	Hebei	116.4855	42.2035	71	Jingjing	Hebei	114.1330	38.0333
32	Fangshan	Beijing	116.0000	39.7000	72	Shijiazhuang	Hebei	114.5418	38.0423
33	Feixiang	Hebei	114.8000	36.5500	73	Tangshan	Tianjin	118.1800	39.6300
34	Fengnan	Hebei	118.1170	39.5500	74	Julu	Hebei	115.0330	37.2167
35	Fengning	Hebei	116.6333	41.2167	75	Kangbao	Hebei	114.6000	41.8500
36	Fengrun	Hebei	118.1000	39.8000	76	Kuancheng	Hebei	118.4830	40.6000
37	Fengtai	Beijing	116.2500	39.8667	77	Laiyuan	Hebei	114.6670	39.3500
38	Fengfeng	Hebei	114.2170	36.4167	78	Langfang	Hebei	116.7000	39.5000
39	Foyeding	Beijing	116.1330	40.6000	79	Yueting	Hebei	118.8833	39.4333
40	Lincheng	Hebei	114.3830	37.4500	80	Zunhua	Hebei	117.9660	40.1892

106

107 This study divided the entire growth period of wheat into six stages: initial growth period,
108 thawing period, wintering period, fast development period, middle growth period, and maturity
109 period. The multi-year average of the development period was used as the local average growth
110 period.

111

2.3 Calculation of potential evapotranspiration

Potential evapotranspiration (ET_0) is the maximum evapotranspiration that a fixed underlying surface can reach when the water supply is not restricted by meteorological factors (Lecina et al., 2003). It determines the dry and wet conditions of the region, along with precipitation, and is a key factor for estimating the ecological water requirement and agricultural irrigation. Further, in the study, the characteristics of the crop are specified, by defining the evapotranspiration of a green grass canopy with the same height, moderate moisture, active growth, and complete coverage of the ground surface with a crop height of 0.12 m, a leaf resistance of 70 s/m, and a reflectivity of 0.23.

ET_0 is based on the daily values of average, maximum and, minimum temperatures, average wind speed, average humidity and sunshine hours. It is calculated using the Penman-Monteith method recommended by FAO (Allen et al., 1998):

$$ET_0 = \frac{0.408\Delta(R_0 - G) + r\frac{900}{T+273}u_2(e_s - e_a)}{\Delta + (1 + 0.34u_2)} \quad (1)$$

In the equation, R_0 is the net radiation on the surface of the canopy (MJ/(m^2·d)); G is the soil heat flux (MJ/(m^2·d)); T is the average temperature (℃); e_s is the saturated vapor pressure (kPa); e_a is the actual vapor pressure (kPa); Δ is the tangent slope of the saturated vapor pressure and temperature curve at T (kPa/℃); r is the hygrometer constant (kPa/℃); u_2 is the wind speed at a height of 2 m (m/s).

2.4 Calculation of effective precipitation

Effective precipitation refers to the precipitation required to balance crop evapotranspiration during the growth period. It is related to the crop water requirement and yearly distribution of precipitation. There are differences in the amount of precipitation that specific crops can use for the same annual precipitation and distribution of different precipitation years, as shown in Figure 2. The crop water requirement that is not met by effective precipitation needs to be supplemented through irrigation, Hence, there is a correlation between effective precipitation and irrigation water requirement.

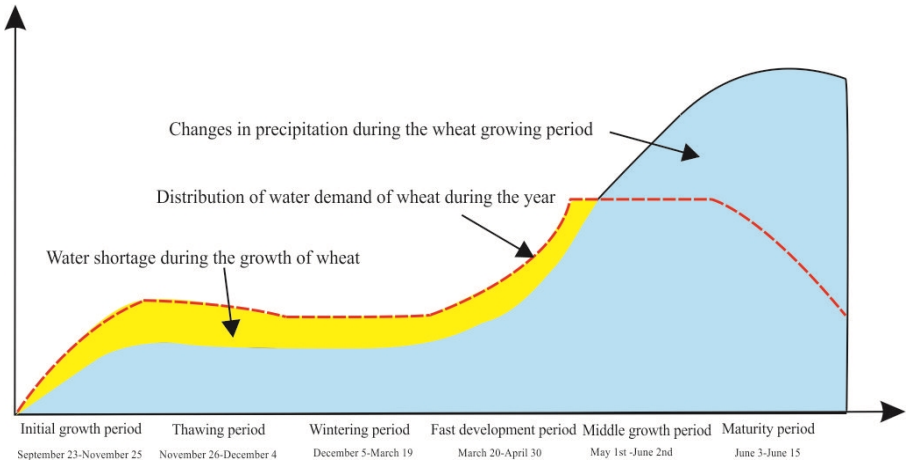

Figure 2 Plot showing the relationship between water requirement and precipitation during wheat growth period

The crop water requirement is determined by the crop coefficient method as follows:

$$ET_C = K_C ET_0 \qquad (2)$$

In the formula, $ET_C$is the crop water requirement (mm/d); $ET_0$is the reference crop evapotranspiration (mm/d); and K_C is the crop coefficient.

The piecewise single-value average crop coefficient method recommended by the Food and Agriculture Organization (FAO), is adopted for K_C. Hence, the variation of K_C during the entire growth period is divided into 6 stages. The values of K_C are shown in Table 2.

Table 2 Wheat crop coefficients for the study area

Wheat	Initial growth period	Thawing period	Wintering period	Fast development period	Middle growth period	Maturity period
Date	September 23-November 25	November 26-December 4	December 5-March 19	March 20-April 30	May 1-June 2	June 3-June 15
K_C	0.6	0.6-0.4	0.4	0.4-1.15	1.15	1.15-0.4

High precipitation occurring in a day may be stored in the soil and subsequently utilized by crops. Thus, effective precipitation can be statistically characterized over time. In this study, the water requirement and characteristics of crop growth every ten days are used for the statistical

calculation of effective precipitation as:

$$\begin{cases} EP_{10d} = ET_C^{10d}, P_{10d} > ET_C^{10d} \\ EP_{10d} = P_{10d}, P_{10d} \le ET_C^{10d} \end{cases} \quad (3)$$

where, $EP_{10d}$is the ten-day scale effective precipitation (mm/10 d); $ET_C^{10d}$is the ten-day crop water requirement (mm/10 d); and$P_{10d}$is the ten-day precipitation (mm/10 d).

The effective precipitation during the crop growth cycle is the sum of the effective precipitation on the ten-day scale:

$$\mathrm{EP} = \sum EP_{10d} \quad (4)$$

2.5 Calculation of irrigation water requirement

A portion of the water needed for agricultural production is obtained from precipitation, and the remaining portion from artificial irrigation. Precipitation is sufficient for crop growth during high-water period, but artificial irrigation is required during low-water period. Therefore, irrigation water requirement, effective precipitation during the crop growth and development stages, the actual area, and the amount of precipitation are closely related factors. Setting the effective precipitation as P_1 and the actual regional precipitation as P_2, the irrigation water requirement, Q can be expressed as

$$\mathrm{Q} = P_2 - P_1 \quad (5)$$

3. Result analysis

3.1 Analysis of climate change characteristics

3.1.1 Rainfall and temperature

The overall precipitation in the Beijing-Tianjin-Hebei region has exhibited a decreasing trend for over two decades, as shown in Figure 3. There is a negative correlation between precipitation and temperature, the correlation coefficient is -0.65. When the precipitation peaks, the temperature shows a dip.

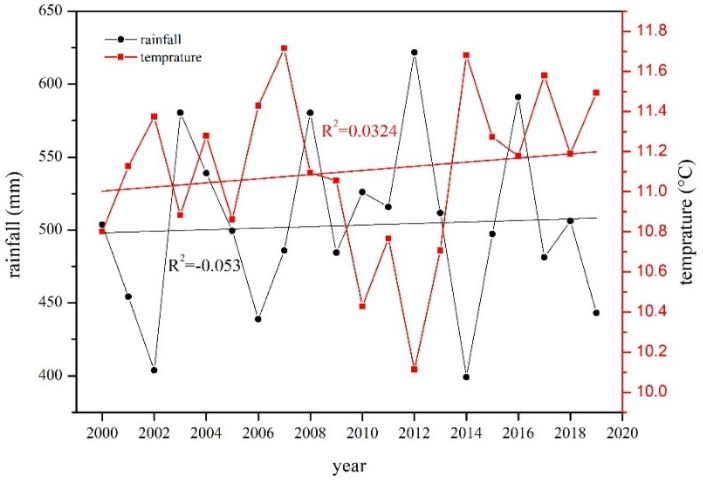

Figure 3 Plot showing the interannual variation trend of rainfall-temperature

3.1.2 Wind speed, radiation, and relative humidity

From the analysis of the multi-year change from the past 20 years in the Beijing-Tianjin-Hebei region, the wind speed has shown a decreasing trend. From 2000 to the present, the multi-year average wind speed was approximately 2.18 m/s. In 2008, the minimum value was 2.05 m/s. The overall range of radiation showed smooth variations, with increasing and decreasing trends in some years; the overall relative humidity showed a downward trend, with a relative humidity change trend (R^2) of 0.359, as shown in Figure 4(c). Analyzed from the spatial change trend, the wind speed was higher in the northern part of the study area, and lower in the transition area between the plain and the mountainous regions. When it reached the southeastern plain, the wind speed gradually increased in the coastal zone, as shown in Figure 5(a), and the humidity gradually increased from the northwest to the southeast. The relative humidity in the hilly area was lower than that of the plain area, and high in the southernmost part of the study area, as shown in Figure 5(b). The average radiation hours were higher in the northwest mountainous area. The spatial radiation variation was high in the Southeast Plain, and relatively low in the southernmost part of the study area, as shown in Figure 5(c). Hence, it can be concluded that relative humidity and radiation are inversely correlated in space; that is, areas with high relative humidity have low radiation, and areas with low relative humidity have high radiation.

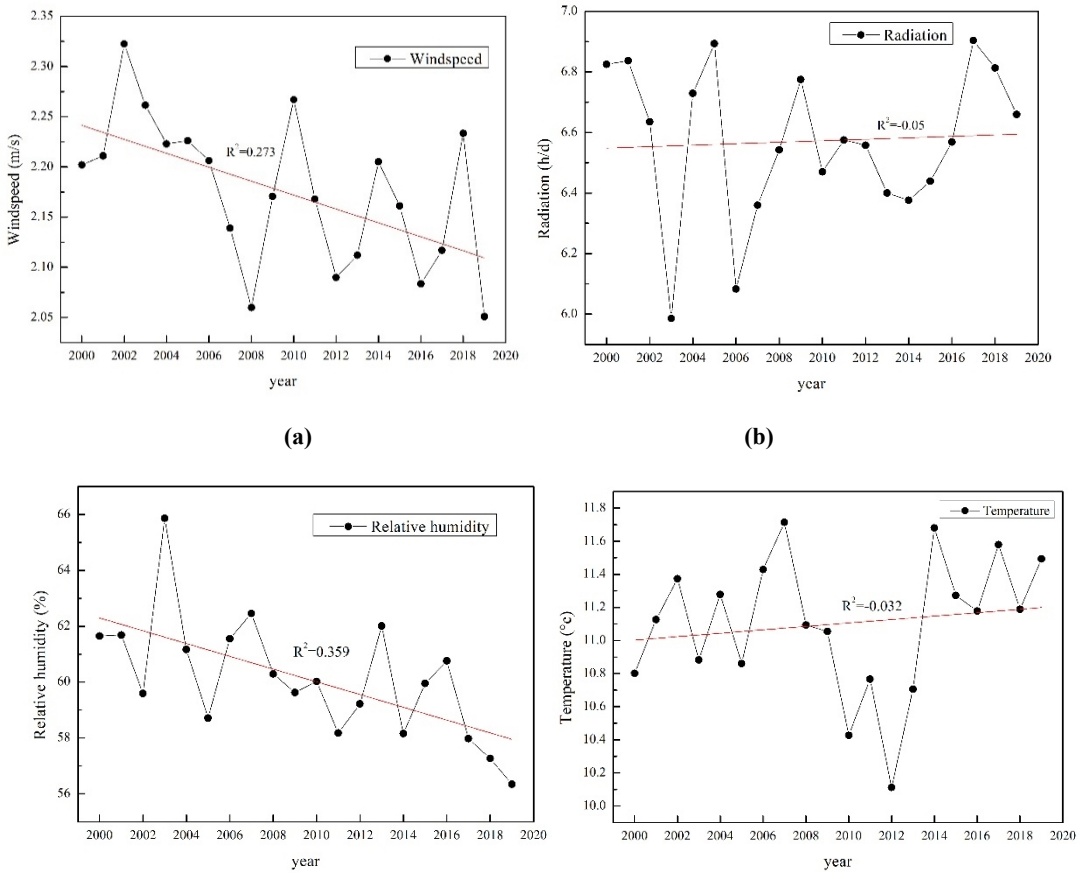

Figure 4 Plot showing the interannual variation trends of (a) wind speed, (b) radiation, (c) relative humidity, and (d) temperature

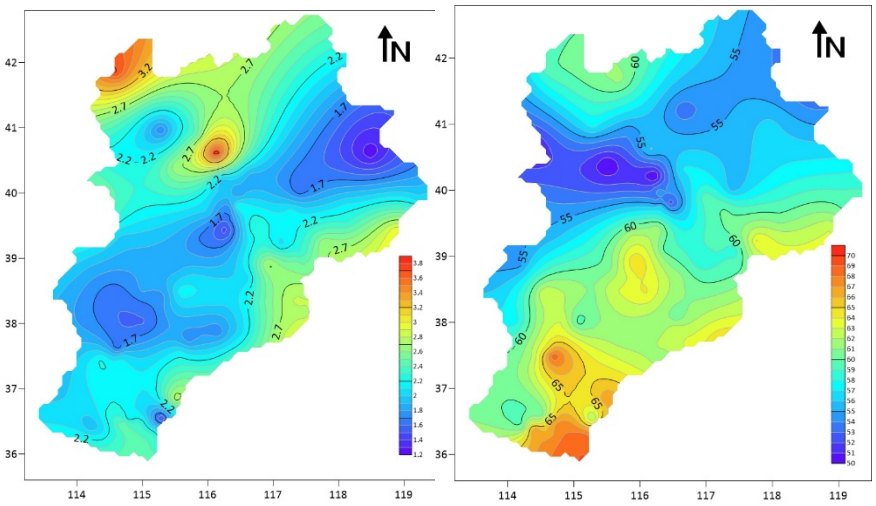

(a) Spatial variation in wind speed (b) Spatial variation in relative humidity

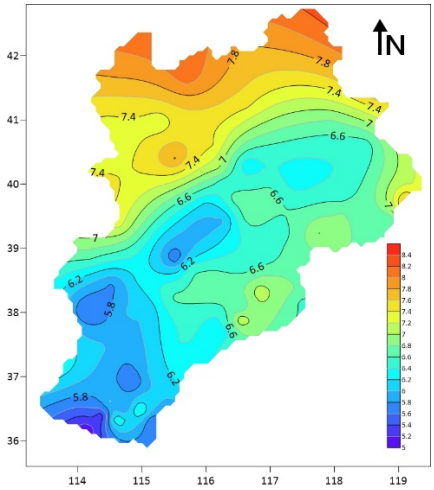

(c) Spatial variation in radiation law

Figure 5 Map showing the characteristic analysis of the meteorological factors

3.2 Distribution characteristics of potential evapotranspiration

Based on the maximum and minimum temperatures, relative humidity, solar radiation, wind speed, and other data from 80 meteorological stations in the Beijing-Tianjin-Hebei region, the potential evapotranspiration of the growth period was calculated using the FAO-98 procedure. The interannual variation of the potential evapotranspiration from 2000 to 2019 is shown in Figure 6. The plot of potential evapotranspiration in the region showed an overall upward trend that declined in certain years. For example, the potential evapotranspiration reached a minimum of 2.82.

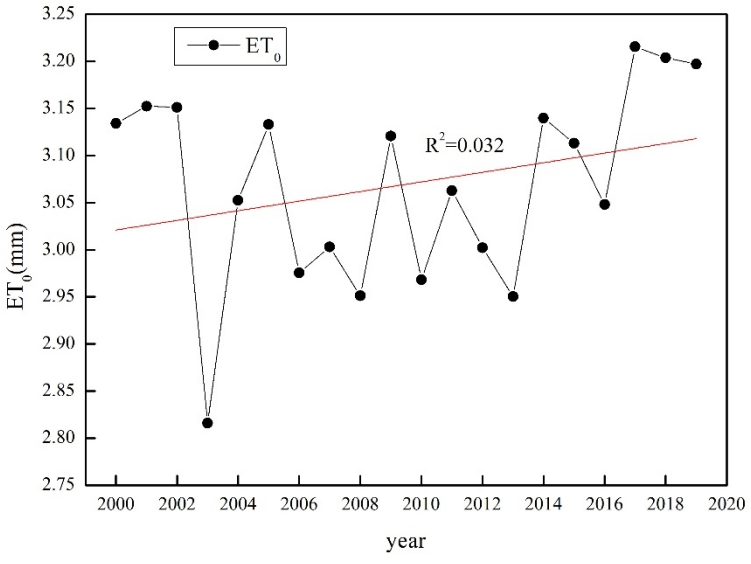

Figure 6 Plot showing the interannual variation of potential evapotranspiration in the growth period

3.3 Distribution characteristics of effective precipitation

The interannual and spatial variations of effective precipitation in the Beijing-Tianjin-Hebei

region from 2000 to 2019 were drawn, using the ten-year scale data of effective precipitation from 80 stations, as shown in Figure 7.

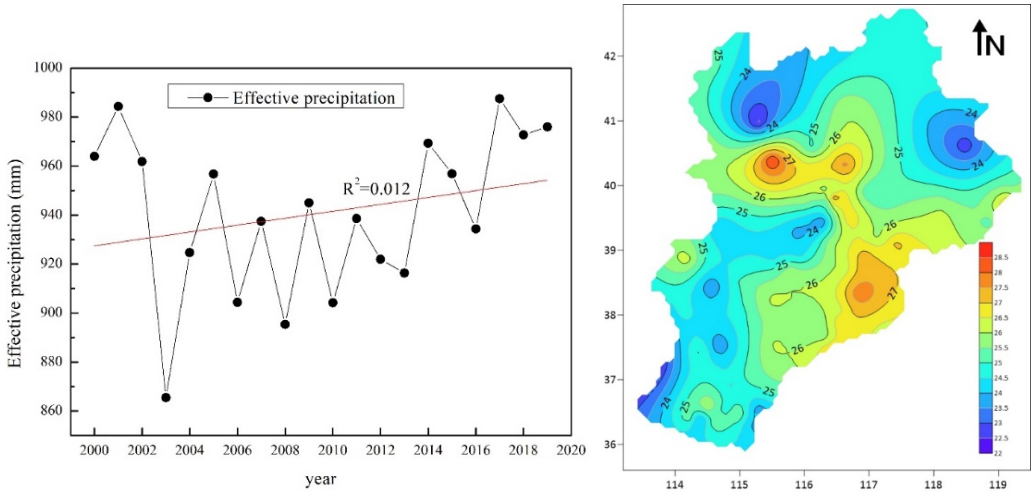

(a) Plot showing the interannual variation of effective precipitation from 2000 to 2019 (b) Map showing the spatial distribution of average effective precipitation from 2000 to 2019

Figure 7 Distribution characteristics of effective precipitation in Beijing-Tianjin-Hebei region

It can be concluded from the figure that the effective precipitation in the Beijing-Tianjin-Hebei region shows an upward trend. From the spatial distribution data of the 10-day average effective precipitation in the Beijing-Tianjin-Hebei region, obvious differences in the effective precipitation in the study area can be observed. In 2000, the effective precipitation was high in the eastern plains and relatively low in the northwest mountainous areas. In 2005, the effective precipitation at the boundary between mountains and plains was significantly low. By 2019, the Beijing-Tianjin-Hebei region had different years. The ten-day average effective precipitation was considerably high in the eastern plain.

3.4 Analysis of irrigation water requirement

3.4.1 Analysis of the change characteristics

The changes in the irrigation water requirement of wheat at 80 sites from 2000 to 2019 were analyzed as shown in Figure 8(a). The overall trend of the plot showing irrigation water requirement of wheat in the study area is flat for most years. Fluctuations can be seen in 2002, 2006, and 2014, when the irrigation water requirement was relatively high or low. Figure 8(b) shows uneven spatial distribution of irrigation water requirement, that is high in the eastern plain and relatively low in the northwest mountainous area.

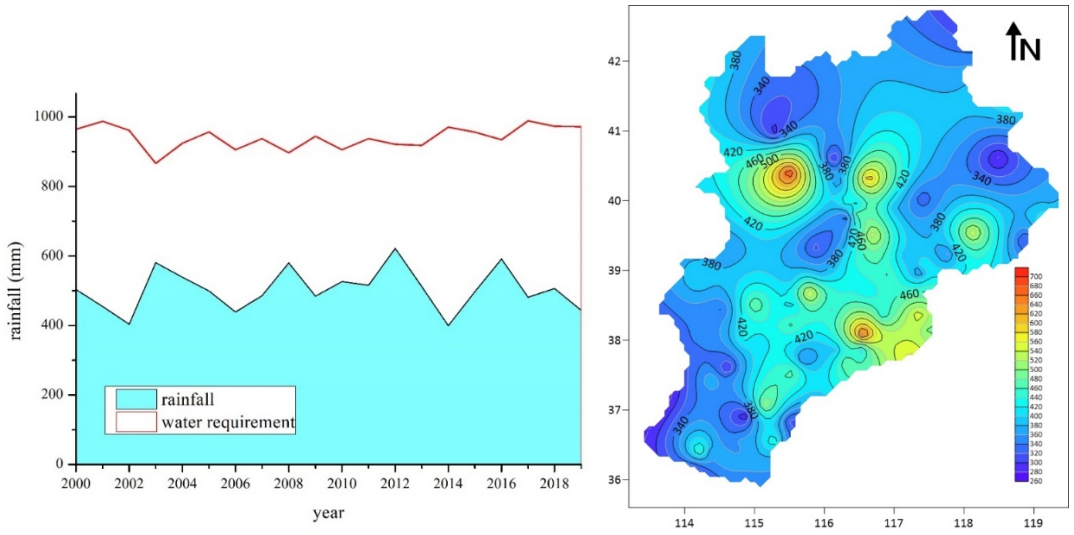

(a) Plot showing the interannual change in irrigation water requirement from 2000 to 2019

(b) Map showing the spatial change in average irrigation water requirement from 2000 to 2019

Figure 8 Distribution characteristics of irrigation water requirement in Beijing-Tianjin-Hebei region

3.4.2 Correlation analysis

The radar chart was used to analyze the changes in irrigation water requirement of wheat from 2000 to 2019, as shown in Figure 9. It can be clearly seen from the shape of the chart that irrigation water requirement in the study area is closest to potential evapotranspiration. However, for individual years, wind speed, relative humidity, and radiation contributions were different. The irrigation water requirement shows positively correlation with potential evapotranspiration, wind speed and radiation changes. The radar chart of the multi-year changes of different meteorological factors in the study area, showed that the overall change in irrigation water requirement has the highest correlation with potential evapotranspiration. However, for individual years, wind speed, relative humidity, and radiation were the common influencing factors affecting regional irrigation

256 water requirement.

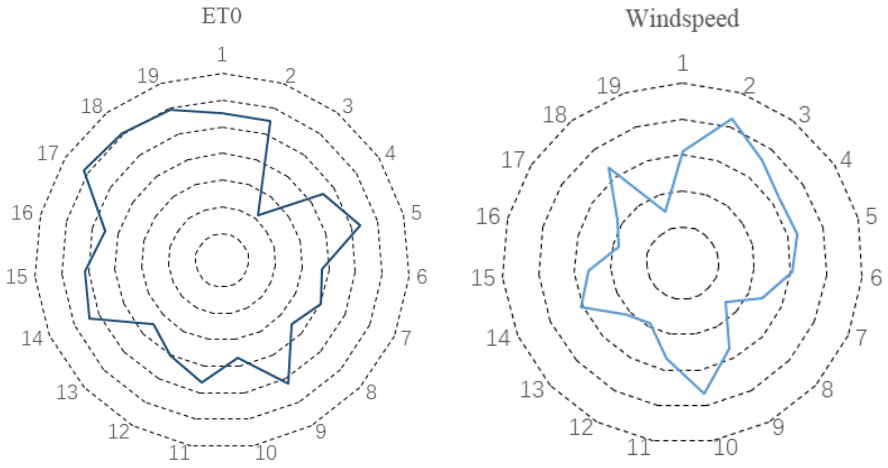

257

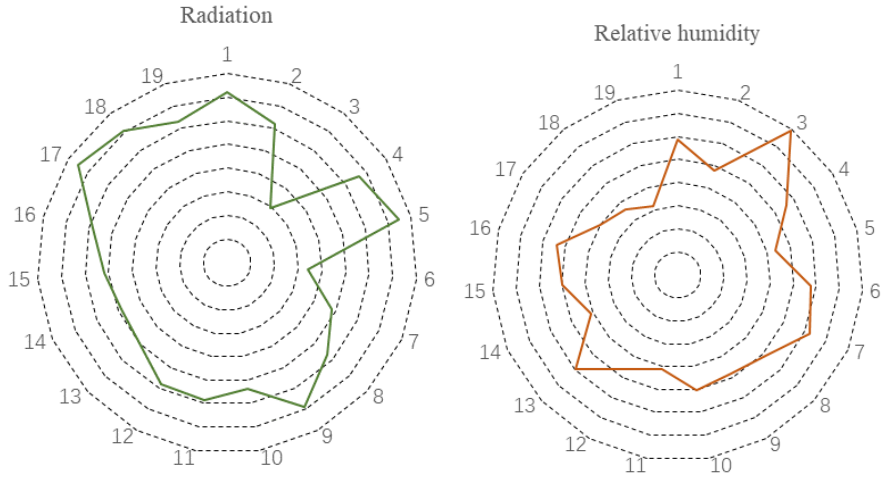

258

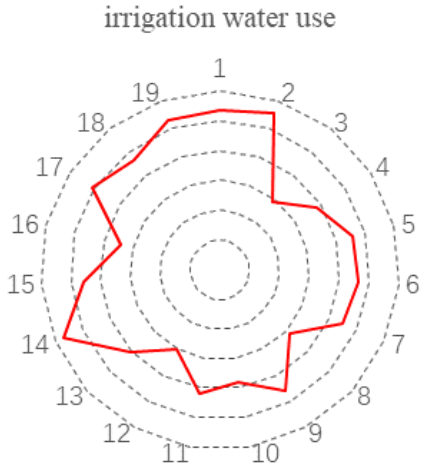

259

260 **Figure 9 Radar chart showing changes in meteorological factors from 2000 to 2019**

261

4. Conclusion and discussion

4.1 Conclusion

(1) The annual average precipitation, average wind speed, and average relative humidity in the Beijing-Tianjin-Hebei region show a general downward trend, while the annual average temperature shows an upward trend. Relative humidity and radiation show negative spatial correlation, that is, areas with high relative humidity have low radiation, and vice versa.

(2) The irrigation water requirement of wheat in the Beijing-Tianjin-Hebei region gradually decreases spatially from north to south and from east to west. The temporal variation in irrigation water requirement in the eastern and western regions shows an opposite trend. The eastern region shows a gradually increasing trend, while the area is decreasing.

(3) Meteorological elements have significant impact on irrigation water requirement. They show negative correlation with irrigation water requirement, potential evapotranspiration, effective precipitation, and relative humidity, and positive correlation with sunshine hours, average temperature, and wind speed. The overall change in irrigation water requirement has the highest correlation with potential evapotranspiration. However, for yearly variations in regional irrigation water requirement, wind speed, relative humidity, and radiation are the common influencing factors.

4.2 Discussion

Irrigation water requirement is affected by complex factors. This study considers the meteorological factors influencing irrigation water requirement in different growth periods of wheat. Potential evapotranspiration and effective precipitation are observed to be the most important indicators that affect irrigation water requirement during the growth period. The effective precipitation during the wheat growth period in the Beijing-Tianjin-Hebei region has increased in the past two decades. This is contrary to the decreasing precipitation trend in the study area, as precipitation in the key growth periods of wheat has significantly increased since the 21st century. The study indicates that irrigation water requirement is affected by several factors at different growth stages of crops. A decrease in sunlight reduces the amount of energy reaching the surface of the Earth, resulting in a decrease in ground evaporation. Furthermore, a decrease in wind speed reduces the rate of water exchange between the air and the soil, affecting the soil moisture balance.

Most previous studies are based on the overall growth period of crops. However, this study

291 focuses on each growth stage of the crop, in combination with meteorological elements and growth
292 period data for comprehensive and accurate analyses. In future studies, these results of irrigation
293 water requirement may be combined with groundwater extraction and artificial channel water
294 transfer in the study area to increase crop yield.

295 Estimating the irrigation water requirement during the growth period of wheat is conducive to
296 the adoption of targeted measures to effectively respond to climate change and increase wheat
297 production. Water can thus be supplemented on time during the critical water requirement period,
298 improving water use efficiency and crop yield.

299 **Availability of data**

300 In this paper, we mainly used the stations data, wheat growth data data to support the findings
301 of this study were supplied by the National Meteorological Information Center (http://data.cma.cn/)
302 under license and so cannot be made freely available.

303 **Author contributions**

304 Xu Chengcheng and Lu Chuiyu designed research; Lu Chuiyu performed research; Xu
305 Chengcheng analyzed data; Wang Jianhhua contributed to interpretation of results; Lu Chuiyu
306 contributed to algorithm development; and Xu Chengcheng wrote the paper.

307 **Competing interests**

308 This manuscript has not been published or presented elsewhere in part or in entirety and is not
309 under consideration by another journal. We have read and understood your journal's policies, and
310 we believe that neither the manuscript nor the study violates any of these. There are no conflicts of
311 interest to declare.

312 **Acknowledgments**

313 We acknowledge reviewers and editors for their patient and valuable advice on improving the
314 quality of this paper and teaching us how to write higher quality papers. We thank our partners from
315 Anhui University of Science and Technology and China Institute of Water Resources and
316 Hydropower Research for their collaborative support during the studies. Financial support for this
317 work was provided by the National Key Research and Development Program of China (grant No.

2016YFC0401404), Applied Technology Research and Development Program of Heilongjiang Province (grant No.GA19C005), National Key Research and Development Program (2016YFC0401300), and the National Science Fund for Distinguished Young Scholars (51625904).

References

Ahmad, R., Zulfiqar, M. (2019). Climate Change-Farmers' Perception, Adaptation and Impact on Agriculture in the Lakki Marwat District of Khyber Pakhtunkhwa. Sarhad Journal of Agriculture, 35(3), 880–889. https://doi.org/10.17582/journal.sja/2019/35.3.880.889

Allen, R.G, Pereira, L.S, Raes, D, et al. Crop evapotranspiration: Guidelines for computing crop water requirements-FAO Irrigation and Drainage Paper 56. Rome: Food and Agriculture Organization of the United Nations, 1998

Bi Yanjie, Zhao Jing, Zhao Yong, Xiao Weihua, & Meng Fanjin. (2020). Spatial-temporal variation characteristics and attribution analysis of potential evapotranspiration in Beijing-Tianjin-Hebei region. Transactions of the Chinese Society of Agricultural Engineering, 36(5), 130–140. https://doi.org/10.11975/j.issn.1002-6819.2020.05.015

Calzadilla, A., Rehdanz, K., Betts, R., Falloon, P., Wiltshire, A., & Tol, R. (2013). Climate change impacts on global agriculture. Climatic Change, 120(1/2), 357–374. https://doi.org/10.1007/s10584-013-0822-4

Chen, C., Greene, A. M., Robertson, A. W., Baethgen, W. E., & Eamus, D. (2013). Scenario development for estimating potential climate change impacts on crop production in the North China Plain. International Journal of Climatology, 33(15), 3124–3140. https://doi.org/10.1002/joc.3648

Dong, Z., Pan, Z., An, P., Wang, J., Zhang, J., Zhang, J., Pan, Y., Huang, L., Zhao, H., Han, G., Fan, D., Wu, D., He, Q., & Pan, X. (2019). A quantitative method for determining the impact threshold of climate change for agriculture. Theoretical & Applied Climatology, 135(1–2), 425–431. https://doi.org/10.1007/s00704-018-2397-5

Geng, X., Wang, F., Ren, W., & Hao, Z. (2019). Climate Change Impacts on Wheat Yield in Northern China. Advances in Meteorology, 1–12. https://doi.org/10.1155/2019/2767018

Guo, J., Huang, G., Wang, X., & Lu, C. (2020). Projections of daily mean surface temperature over the Beijing-Tianjin-Hebei region through a stepwise cluster downscaling method. Theoretical & Applied Climatology, 141(1/2), 71–86. https://doi.org/10.1007/s00704-020-03172-w

347 Guo, X., Ren, D., & Li, C. (2020). Study on the problem of wind power curtailment in Beijing-Tianjin-
348 Hebei based on risk-return. Energy Sources Part A: Recovery, Utilization & Environmental
349 Effects, 42(21), 2632–2647. https://doi.org/10.1080/15567036.2019.1618977
350 Iglesias, A., Quiroga, S., Moneo, M., & Garrote, L. (2012). From climate change impacts to the
351 development of adaptation strategies: Challenges for agriculture in Europe. Climatic
352 Change, 112(1), 143–168. https://doi.org/10.1007/s10584-011-0344-x
353 IPCC 1990. Climate Change and Impact 1990.Cambridge University Press, Cambridge.
354 IPCC 1996.Climate Change 1995. Impacts, Adaptation, and Mitigation. Cambridge University
355 Press, Cambridge.
356 IPCC 2001. Climate Change 2001. Impacts, Adaptation, and Vulnerability. Cambridge University
357 Press, Cambridge.
358 IPCC 2007. Climate change 2007: the physical science basis.Cambridge University Press,
359 Cambridge.
360 IPCC 2013. Climate change 2013: the physical science basis. Cambridge University Press,
361 Cambridge.
362 Ju, H., Velde, M., Lin, E., Xiong, W., & Li, Y. (2013). The impacts of climate change on agricultural
363 production systems in China. Climatic Change, 120(1/2), 313–324.
364 https://doi.org/10.1007/s10584-013-0803-7
365 Lecina, S., Martínez-Cob, A., Pérez, P. J., Villalobos, F. J., & Baselga, J. J. (2003). Fixed versus
366 variable bulk canopy resistance for reference evapotranspiration estimation using the Penman–
367 Monteith equation under semiarid conditions. Agricultural Water Management, 60(3), 181.
368 https://doi.org/10.1016/S0378-3774(02)00174-9
369 Liu, J., Folberth, C., Yang, H., Röckström, J., Abbaspour, K., & Zehnder, A. J. B. (2013). A Global and
370 Spatially Explicit Assessment of Climate Change Impacts on Crop Production and Consumptive
371 Water Use. PLoS ONE, 8(2), 1–13. https://doi.org/10.1371/journal.pone.0057750
372 Lv, Z., Liu, X., Cao, W., & Zhu, Y. (2013). Climate change impacts on regional wheat production in
373 main wheat production regions of China. Agricultural & Forest Meteorology, 171–172, 234–248.
374 https://doi.org/10.1016/j.agrformet.2012.12.008
375 Mayank, Parveen, S., Sharma, A., & Mohit. (2019). Perception about changes in Climate and Potential

376 impact of such changes on Ecosystems, Biodiversity, Agriculture and Livelihoods at local level in
377 Jhansi district of Bundelkhand region of Uttar Pradesh. International Journal of Pharmacy & Life
378 Sciences, 10(4), 6198–6215.
379 McBride, L. A., P. Hope, A., Canty, T. P., Bennett, B. F., Tribett, W. R., & Salawitch, R. J. (2020).
380 Comparison of CMIP6 Historical Climate Simulations and Future Projected Warming to an
381 Empirical Model of Global Climate. Earth System Dynamics Discussions, 1–59.
382 https://doi.org/10.5194/esd-2020-67
383 Men, B., Wu, Z., Liu, H., Tian, W., & Zhao, Y. (2020). Spatio-temporal Analysis of Precipitation and
384 Temperature: A Case Study Over the Beijing–Tianjin–Hebei Region, China. Pure & Applied
385 Geophysics, 177(7), 3527–3541. https://doi.org/10.1007/s00024-019-02400-3
386 Noufé, D., Mahé, G., Kamagaté, B., Servat, É., Goula Bi Tié, A., & Savané, I. (2015). Climate change
387 impact on agricultural production: the case of Comoe River basin in Ivory Coast. Hydrological
388 Sciences Journal/Journal Des Sciences Hydrologiques, 60(11), 1972–1983.
389 https://doi.org/10.1080/02626667.2015.1032293
390 Pons, C., Voß, A., Schweiger, R., & Müller, C. (2020). Effects of drought and mycorrhiza on wheat
391 and aphid infestation. Ecology & Evolution (20457758), 10(19), 10481–10491.
392 https://doi.org/10.1002/ece3.6703
393 Seo, S. N. (2013). An essay on the impact of climate change on US agriculture: weather fluctuations,
394 climatic shifts, and adaptation strategies. Climatic Change, 121(2), 115–124.
395 https://doi.org/10.1007/s10584-013-0839-8
396 Schönhart, M., Schauppenlehner, T., Kuttner, M., Kirchner, M., & Schmid, E. (2016). Climate change
397 impacts on farm production, landscape appearance, and the environment: Policy scenario results
398 from an integrated field-farm-landscape model in Austria. Agricultural Systems, 145, 39–50.
399 https://doi.org/10.1016/j.agsy.2016.02.008
400 Song, X., Zhang, C., Zhang, J., Zou, X., Mo, Y., & Tian, Y. (2020). Potential linkages of precipitation
401 extremes in Beijing-Tianjin-Hebei region, China, with large-scale climate patterns using wavelet-
402 based approaches. Theoretical and Applied Climatology, 141(3/4), 1251–1269.
403 https://doi.org/10.1007/s00704-020-03247-8
404 Sun, S., Wu, P., Wang, Y., Zhao, X., Liu, J., & Zhang, X. (2013). The impacts of interannual climate

405 variability and agricultural inputs on water footprint of crop production in an irrigation district of
406 China. Science of the Total Environment, 444, 498–507.
407 https://doi.org/10.1016/j.scitotenv.2012.12.016
408 Van der Geest, K., Warner, K. (2020). Loss and damage in the IPCC Fifth Assessment Report
409 (Working Group II): a text-mining analysis. Climate Policy (Earthscan), 20(6), 729–742.
410 https://doi.org/10.1080/14693062.2019.1704678
411 Wang, G., Li, T., Zhang, W., & Yu, Y. (2014). Impacts of Agricultural Management and Climate Change
412 on Future Soil Organic Carbon Dynamics in North China Plain. PLoS ONE, 9(4), 1–10.
413 https://doi.org/10.1371/journal.pone.0094827
414 Wang, Z., Meng, C., Chen, J., & Chen, F. (2019). Risk Assessment of Crop Production Amid Climate
415 Change Based on the Principle of Maximum Entropy: A Case Study of Wheat Production on the
416 North China Plain. International Journal of Plant Production, 13(4), 275–284.
417 https://doi.org/10.1007/s42106-019-00053-9
418 Weerathunga, W. A. M. T., Rajapaksa, G. (2020). The impact of elevated temperature and CO^2 on
419 growth, physiological and immune responses of Polypedates cruciger (common hourglass tree
420 frog). Frontiers in Zoology, 17(1), 1–25. https://doi.org/10.1186/s12983-019-0348-3
421 Zhang, B., Fan, Z., Du, Z., Zheng, J., Luo, J., Wang, N., & Wang, Q. (2020). A Geomorphological
422 Regionalization using the Upscaled DEM: the Beijing-Tianjin-Hebei Area, China Case
423 Study. Scientific Reports, 10(1), 1–12. https://doi.org/10.1038/s41598-020-66993-9
424 Zhenyu Han,Ying Shi,Jia Wu. (2019). Combined Dynamical and Statistical Downscaling for High-
425 Resolution Projections of Multiple Climate Variables in the Beijing–Tianjin–Hebei Region of
426 China. Journal of Applied Meteorology and Climatology, 58(11), 2387–2403.
427 https://doi.org/10.1175/JAMC-D-19-0050.1
428 Zhang, Q., Gu, X., Singh, V. P., Liu, L., & Kong, D. (2016). Flood-induced agricultural loss across China
429 and impacts from climate indices. Global & Planetary Change, 139, 31–43.
430 https://doi.org/10.1016/j.gloplacha.2015.10.006